


Peter L. Kaskiewicz¹
Thomas D. Turner¹
Nicholas J. Warren¹
Colin Morton²
Peter J. Dowding²
Neil George³
Kevin J. Roberts^{1,*}

Isothermal by Design: Comparison with an Established Isothermal Nucleation Kinetics Analysis Method

The nucleation kinetics of the alpha form of *p*-aminobenzoic acid from ethanolic and aqueous solutions is examined through a comparative examination of temperature-jump and anti-solvent down-out isothermal crystallization methodologies. Analysis of the data reveals the measured induction times, and the calculated effective interfacial tensions as a function of the supersaturation show broadly equivalent behavior for the aqueous-ethanol mixed-solvent down-out and temperature-jump ethanol solution systems, confirming the comparability of the two methodologies. The results also demonstrate poorer agreement with the temperature-jump pure aqueous system, highlighting the importance of the strength of solvation/desolvation as the key rate-limiting process for the overall nucleation behavior.

 This is an open access article under the terms of the Creative Commons Attribution License, which permits use, distribution and reproduction in any medium, provided the original work is properly cited.

Keywords: Antisolvent crystallization, Induction time, Isothermal, Kinetics, Nucleation

Received: March 06, 2020; *revised:* July 07, 2020; *accepted:* July 09, 2020

DOI: 10.1002/ceat.202000113

1 Introduction

Isothermal by design (IbD) [1] is an antisolvent crystallization methodology for studying solution phase nucleation kinetics; it has been shown to be applicable over a wide range of supersaturations (*S*), particularly accessing supersaturations that can be challenging to attain through conventional temperature-jump cooling-based isothermal crystallization methodologies. Whilst IbD has been shown to enable key nucleation kinetic information to be determined [1], such data has not, as of yet, been directly cross-correlated with those obtained by using temperature-jump isothermal methodology (TJM) for the same crystallization system.

TJM is a prominent methodology for assessing nucleation kinetics and has been used extensively and successfully to understand how crystallization solution systems nucleate [2–6]. It involves cooling an undersaturated solution to a given level of supersaturation, and the time it takes to crystallize from this set point is taken as the induction time (τ), which is a combination of three time components: the relaxation time for molecular cluster distribution, the time to form a stable nucleus, and the time for growth to a detectable size (τ_d , τ_n , and τ_g , respectively)¹⁾ [7]. However, difficulties in achieving relatively high levels of solution supersaturation through this methodology are created due to the initial cooling required to achieve a certain solution supersaturation, which can impact on the induction time and as such affect the calculation of the associated nucleation kinetics.

In contrast, IbD utilizes an antisolvent methodology, whereby a miscible second solvent is added to a solution, which lowers the solubility of a given solute, increasing the level of supersaturation and therefore the rate of nucleation (*J*), following the relationship $J \propto S$. This relationship is outlined through the classical nucleation theory (CNT), which is the crystallization analysis pathway used in this study for IbD and TJM. However, the enthalpy of mixing associated with the addition of a second miscible solvent to a solution can cause a change in the solution temperature. IbD takes account for this through simple antisolvent calorimetry calibrations, whereby the antisolvent temperature is offset to ensure that the desired solution temperature is maintained, enabling the same analysis methodology to be undertaken as with TJM.

This work focusses on a comparison of nucleation kinetic data obtained through IbD and TJM, detailing the advantages and drawbacks of both techniques, while comparing the results obtained through IbD with those from TJM over a similar supersaturation range. Results from IbD are obtained from a

¹Peter L. Kaskiewicz, Dr. Thomas D. Turner, Dr. Nicholas J. Warren, Prof. Kevin J. Roberts
K.J.Roberts@leeds.ac.uk
University of Leeds, School of Chemical and Process Engineering, Leeds LS2 9JT, UK.

²Dr. Colin Morton, Prof. Peter J. Dowding
Infineum UK Ltd., Milton Hill Business and Technology Centre, Abingdon, UK.

³Dr. Neil George
Syngenta UK Ltd., Jealott's Hill International Research Centre, Bracknell, Berkshire, UK.

1) List of symbols at the end of the paper.

previous study focusing on the crystallization of *para*-aminobenzoic acid (pABA) from ethanol/water (EtOH/H₂O) mixed-solvent solutions [1], while those from TJM are a combination of work from a previous study for pABA in EtOH [6, 8] and H₂O solutions [8]. The system choice of pABA from these solvent systems represents a well-studied model pharmaceutical compound used in many crystallization processes.

2 Materials and Methods

2.1 Materials

pABA (99% purity) was supplied by Alfa Aesar and Sigma, ethanol absolute ($\geq 99.8\%$ purity) was supplied by VWR, and deionized water was sourced on site at the University of Leeds.

2.2 Experimental Procedure

All TJM and IbD crystallization experiments were performed on the Technobis Crystal16 system [9] at the 1-mL scale with magnetic stirring.

2.2.1 TJM

The TJM induction time experiments were performed by initially preparing solutions with concentrations of 180 and 200 g kg⁻¹, for pABA in EtOH solutions, and 6 and 8 g kg⁻¹, for pABA in H₂O solutions. The measurements were carried out at values of supersaturation ranging from 1.03 to 1.10 (solution temperatures: 299–303 K) and 1.07 to 1.15 (solution temperatures: 303–307 K), respectively, for EtOH solutions, and 1.17 to 1.27 (solution temperatures: 296–298 K) and 1.17 to 1.32 (solution temperatures: 302–305 K), respectively, for H₂O solutions. The values of supersaturation were calculated using solubility data collected from Turner [8] and Turner et al. [10]. Solutions were then heated to 10 K above the dissolution temperature and held for 1 h to ensure complete dissolution of the solute. Solutions were then subjected to rapid cooling at 5 K min⁻¹ to the desired holding temperature within the metastable zone width. The measured induction times were taken as the difference from the start time after reaching the set solution temperatures to the time of the measured transmittance decrease, from 100% to below 90%, indicating crystallization. Experiments at each level of supersaturation were repeated eight times at the relevant concentration to provide an average induction time measurement.

2.2.2 IbD

The IbD experiments were performed over a large compositional range of pABA in EtOH/H₂O mixed solutions, with five solution temperatures, from 293 to 301 K in 2-K increments, denoting the temperatures at which nucleation occurred using this methodology. Initial solutions were prepared with a pABA saturation concentration of 293 K in an EtOH/H₂O 70:30 wt %

solution, with the composition chosen based on solubility data. Solubility was determined over the full solvent compositional range, with 11 solvent compositions ranging in 10-wt % increments of EtOH from pure EtOH to pure H₂O used. The solutions were decanted into 1.5-mL glass vials in varying volumes, from 0.2 to 0.8 mL, which would be made up to 1 mL in volume after addition of H₂O antisolvent, with a 1-mL needle and syringe. This addition methodology would result in minor volume variations in antisolvent addition; however, these were assumed to have a negligible effect on the induction times in comparison to the innate variability obtained for the induction time results for repeats of the same solution composition.

Antisolvent calorimetry calibrations were performed, following the workflow outlined in Kaskiewicz et al. [1], to ensure that the exothermic heating effect caused upon H₂O addition to the pABA solution was nullified. Calorimetry calibrations were performed by varying the antisolvent temperature and measuring the solution temperature after antisolvent addition at each selected solution temperature, over a range of initial solution volumes. Plots of antisolvent temperature versus final solution temperature were made and linear regression models fitted in order to determine the antisolvent temperature required to maintain the solution temperature and to ensure an isothermal antisolvent addition process. This was subsequently tested to ensure that isothermal conditions were maintained upon antisolvent addition at the determined required antisolvent temperatures, with minimal deviation in temperature changes found.

Following the calorimetry calibrations, induction time experiments were performed over the full range of initial solution volumes, varying in 0.05-mL increments, using the five solution temperatures previously described and the calibrated antisolvent temperatures. Values of induction time were determined using transmission data, in the same manner as the TJM experiments, but the onset of supersaturation was determined through an initial change in transmission upon antisolvent addition, followed by a return to 100% transmission after mixing, which denoted the time zero for the induction time measurements, which took around 1–2 s to achieve after mixing. Given the low solution volumes used and the high degree of mixing induced by the antisolvent addition method, this was deemed to be sufficient time for the solutions to mix and homogenize. Experiments were repeated 16 times for each initial solution volume and temperature to provide an average induction time measurement.

A full description of the methodology used to determine the solubility and to perform all stages of the IbD methodology is provided elsewhere [1].

2.2.3 Nucleation Kinetics Analysis

Molar supersaturations for each solution were calculated according to

$$S = \frac{c}{c^*} \quad (1)$$

where c is the absolute solute concentration and c^* is the saturation concentration.

The rate of nucleation was taken to be related to the induction time obtained from the experiments, under the relationship described through Eq. (2) [7]:

$$\tau \propto J^{-1} \quad (2)$$

The induction time data (τ as a function of S) were analyzed using the classical nucleation theory (CNT) [11, 12], according to:

$$\ln \left\{ \tau \left[S(S-1)^{md} \right]^{\frac{1}{1+md}} \right\} = \ln k_{\text{md}} + \frac{B}{[(1+md)(kT \ln S)^2]} \quad (3)$$

where

$$k_{\text{md}} = \frac{1}{\left[\frac{k_v z f_e^* c_s d_0^d f_{e,s}^{\text{md}}}{(1+md)} \right]} \quad (4)$$

$$B = \frac{16\pi v_0^2 \gamma_{\text{eff}}^3}{3kT} \quad (5)$$

where m is the crystallite growth exponent, with $m=1$ for pABA, indicating growth through diffusion of solute through a stagnant layer around the crystal [13], d is related to the dimensionality of crystal growth, with $d=1$ for pABA due to its needle-like morphology, k is the Boltzmann constant, α_{det} is the fraction of detectable crystallized volume and is equal to V_c/V , where V_c is the crystallized volume and V is the solution volume, k_v is the crystallite growth shape factor, z is the Zeldovich factor, f_e^* is the frequency of monomer attachment to the nucleus at $\Delta\mu=0$, c_s is the concentration of sites in the system on which clusters of the new phases can form, d_0 is the molecular diameter $\approx \left(\frac{6v_0}{\pi}\right)^{1/3}$, $f_{e,s}$ is the frequency of molecular attachment per growth site at $\Delta\mu=0$, v_0 is the volume occupied by a solute molecule in a crystal, and γ_{eff} is the effective interfacial tension. A full derivation of Eq. (3) is given in a previous research article [4].

For all solutions studied using TJM and solution compositions (initial starting solution volume) ranging from 24 to 8 mol% EtOH for IbD studies, plots of $\ln \left\{ \tau \left[S(S-1)^{md} \right]^{\frac{1}{1+md}} \right\}$ versus $\frac{1}{T^3(\ln S)^2}$ were constructed, over the range of temperatures used to study each individual solution composition. This provided data for varying supersaturation with constant solution composition, and a linear regression was fitted to the data, with the slope equating to $\frac{16\pi v_0^2 \gamma_{\text{eff}}^3}{3(1+md)k^3}$, enabling the calculation of γ_{eff} . This parameter could not be determined for solution compositions of 31 and 27 mol% EtOH using IbD, due to a limited number of data points over a substantial temperature range, which prohibited an accurate calculation of the effective interfacial tension in this compositional range. The intercept of the linear regression was equal to $\ln k_{\text{md}}$. From the slope, the critical nucleus radius (r^*) and the number of molecules in the critical nucleus (i^*) were calculated, according to:

$$r^* = \frac{2\gamma_{\text{eff}} v_0}{kT \ln S} \quad (6)$$

$$i^* = \frac{4\pi r^{*3}}{3v_0} \quad (7)$$

Also, $(\log S)^{-2}$ was plotted as a function of $\log \tau$, given the relationship:

$$\log \tau \propto \left[\frac{\gamma_{\text{eff}}^3}{T^3 (\log S)^2} \right] \quad (8)$$

with any changes in the trend of data over a single temperature resulting in large increases in the linear regression fit of data, suggesting a change in the nucleation mechanism from heterogeneous nucleation (HEN), at lower supersaturations, to homogeneous nucleation (HON), at higher supersaturations [7, 14, 15].

3 Results and Discussion

3.1 IbD Calorimetry Calibrations

Fig. 1 displays calorimetry calibration data collected from pABA in mixed EtOH/H₂O solutions held at 297 K, with different antisolvent addition temperatures over a range of initial solution volumes [1]. The antisolvent temperature was found to have a significant effect on the final solution temperature, which, for example, can be seen by a required antisolvent temperature of > 20 K lower than that of the solution temperature for a 0.8-mL initial solution volume, in order to maintain the solution temperature at 297 K.

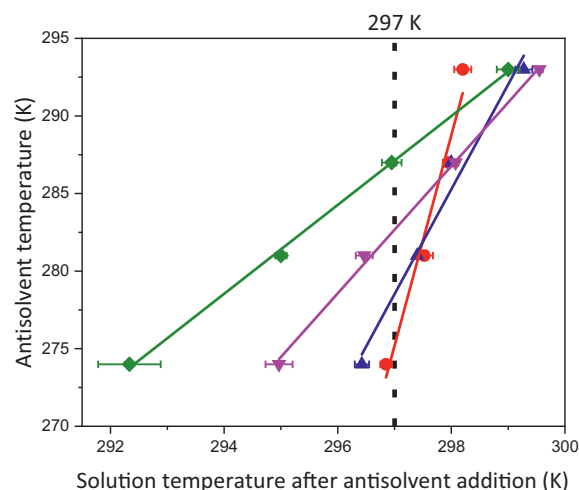


Figure 1. Effect of the antisolvent temperature on solutions of the pABA-in-EtOH/H₂O mixed-solvent system held at constant temperature (297 K). Effect of the antisolvent temperature on 0.3 mL initial solution (green diamonds), 0.5 mL initial solution (pink down-pointing triangles), 0.65 mL initial solution (blue up-pointing triangles), and 0.8 mL initial solution (red circles), shown by the gradients of the linear relationships. The dotted line shows the solution temperature prior to antisolvent addition [1].

This substantial variation in required antisolvent temperature, when compared to the solution temperature, as well as the large difference in the required antisolvent temperature with different addition quantities, demonstrates the importance for offsetting the antisolvent temperature for antisolvent crystallization processes. Therefore, understanding the system as a whole to ensure that accurate and precise measurements are taken, creating reliable data for which to analyze, is extremely important.

3.2 Induction Time Measurements

Induction time data were collected as a function of supersaturation for pABA in pure EtOH and pure H₂O solvents under TJM and for a range of compositions under IbD, from 31:69 to 11:89 mol % EtOH/H₂O, respectively, as highlighted in Fig. 2.

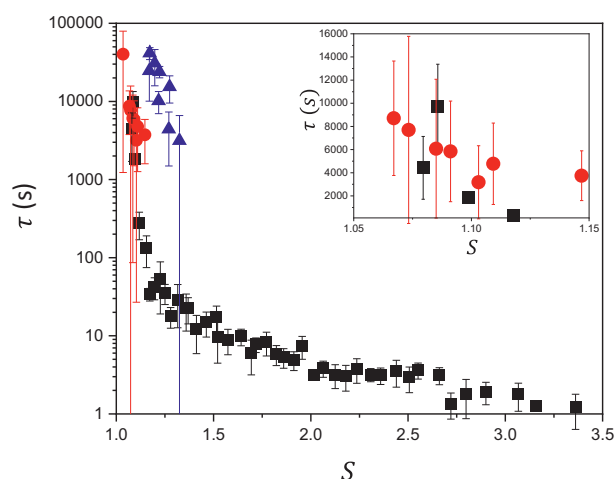


Figure 2. Supersaturation versus induction time data collected from pABA in EtOH solutions at concentrations of 180 and 200 g kg⁻¹ (red circles), pABA in water solutions at 6 and 8 g kg⁻¹ (blue triangles), and IbD experiments over the full range of concentrations, compositions, and supersaturations [1] (black squares). Standard deviations of repeats are displayed. τ -axis in log format. Inset shows data collected for 100 s < τ < 16 000, from 1.0 < S < 1.15.

A comparison of the collected data demonstrates the ability of the IbD methodology to enable the collection of induction time data at higher levels of supersaturation compared to TJM. This is extremely useful for potential accelerated testing capabilities, allowing higher rates of nucleation to be attained, and also for understanding the crystallization process at high supersaturation. For reliable induction time data under TJM, the cooling time to reach the set level of supersaturation must be negligible with respect to the induction time, ensuring that the time to cool has no real impact on the determined induction time value. However, if the cooling time increases and as such the induction time decreases, the cooling time can have a significant effect on the induction time, making results unreliable. Therefore, this limits the achievable level of supersaturation using TJM and as such makes it less effective under these solution conditions. For example, for a pABA in EtOH solution at

a concentration of 180 g kg⁻¹, in order to achieve S=1.3, it would take 306 s of idealized linear cooling at the rate of 5 K min⁻¹ from the saturation temperature. However, the results obtained through IbD demonstrate that, at this level of supersaturation, the induction time would only be around 20 s, over 15 times shorter than the time to cool. It is clear that the time to cool would be much longer than the induction time and so would have a substantial effect on it, rendering it unreliable. It would also be unlikely that the solution could reach this level of supersaturation, given that the cooling time is so long compared to the induction time. This is further exacerbated by the fact that a high cooling rate of 5 K min⁻¹ was used for the 1-mL solutions in this study, but this cooling rate would not be achievable if the solution volume was scaled up, such as to a manufacturing scale, which would potentially create an even longer cooling period and, as such, a lower achievable level of supersaturation.

What is further evident from the τ -versus-S data is that the reproducibility of the results decreases at lower levels of supersaturation. This can be seen with an increase in the coefficient of variation as the induction time increased (Fig. 3). This might be due to a number of factors, such as: minor changes in supersaturation having a large effect on the induction time caused with temperature control systems, also, any “foreign” particulates within the solution vials impacting upon the nucleation process through a heterogeneous nucleation mechanism and, importantly, the fact that the process of nucleation is stochastic, which can lead to large variations in induction time results for the same experiment, even if all experimental conditions remained consistent. This aspect has led, in other studies [2], to the use of a large number of experimental repeats (~80 repeats for each supersaturation), requiring the application of probability distribution functions to analyze the induction time data. This requires a large number of experiments to be carried out, and remains, experimentally, a time-consuming process. At the higher levels of supersaturation accessible through IbD, coefficients of variation were found to be lower, due to a higher

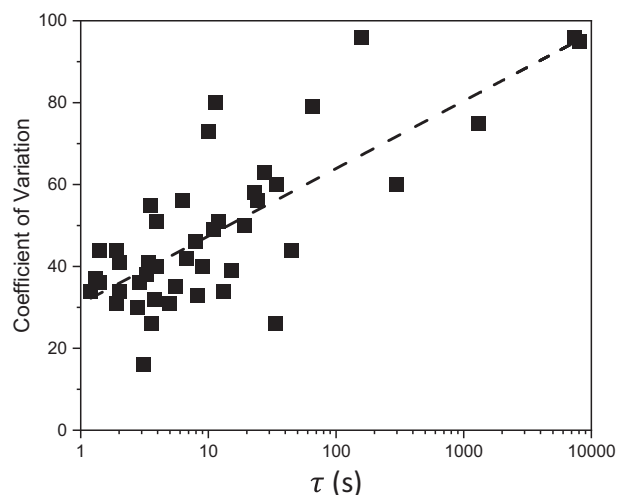


Figure 3. Coefficient of variation calculated for the IbD experiments, as a function of the induction time. The dashed line shows the linear regression fitted to data.

driving force to nucleation somewhat overcoming the stochasticity of nucleation. This is highly beneficial as it indicates data with an increase in reproducibility and it provides more confidence in results obtained through analysis of induction time data at these levels of supersaturation.

The results obtained from the TJM and IbD methodologies also demonstrate that the mixed-solvent solutions used with IbD follow a similar trend to results obtained for pABA in pure EtOH solutions, but not those obtained for pABA in pure H₂O solutions. A higher level of supersaturation was found to be required for the nucleation of pABA in H₂O solutions, for a similar induction time to those of the other systems in this study. The mixed-solvent solutions used with the IbD methodology ranged in composition from 8 to 25 mol % EtOH, meaning that all solutions had a higher H₂O content compared to EtOH. However, despite this, these solutions were found to follow a similar τ -versus- S trend as those of the pABA in EtOH solutions, which could be due to the strong solvation power of EtOH. EtOH molecules have both hydrophobic (alkyl) and hydrophilic (alcohol) moieties and, hence, are able to solvate the polar and apolar electronic components of the pABA molecule. In contrast, for H₂O, much of the surface area of the pABA molecules is largely inaccessible due to the hydrophobic nature of the benzene ring, and therefore this solvent system has much weaker solvation properties and as such a much lower solubility [10, 16, 17]. This means that, although much lower amounts of EtOH are in solution, EtOH molecules could dominate the solvation process. This aspect would be consistent with pABA in mixed EtOH/H₂O solvent solutions, used with IbD, being similar in nucleation properties to pABA in EtOH solutions, as studied using TJM.

The similar trend at low supersaturation of pABA in EtOH solutions to the mixed-solvent solutions suggests that it may be possible to extrapolate data obtained from the mixed-solvent solutions used through IbD to a single-solvent system that is being studied for accelerated testing. Therefore, it may be possible to probe a high level of supersaturation to accelerate a very slow nucleating system and determine how the system behaves at low supersaturation conditions. The data also provides validity with the IbD results, as data collected in the same range of supersaturation had similar induction time values, shown by the inset in Fig. 2.

3.3 Nucleation Kinetic Parameters

3.3.1 Effective Interfacial Tension

An example plot for the determination of the effective interfacial tension for pABA in H₂O solution at 6 g kg⁻¹ is shown in Fig. 4. A comparison of calculated effective interfacial tension values from the different methodologies shows a stark difference between those calculated through TJM and IbD (Tab. 1). Given that the effective interfacial tension is strongly influenced by the solvent environment, this result is expected. The effective interfacial tension calculated from IbD compares well to a previous study performed by Jiang and ter Horst [2], which studied a very similar compound, *m*-aminobenzoic acid, using the same solvent composition that was used for IbD, a

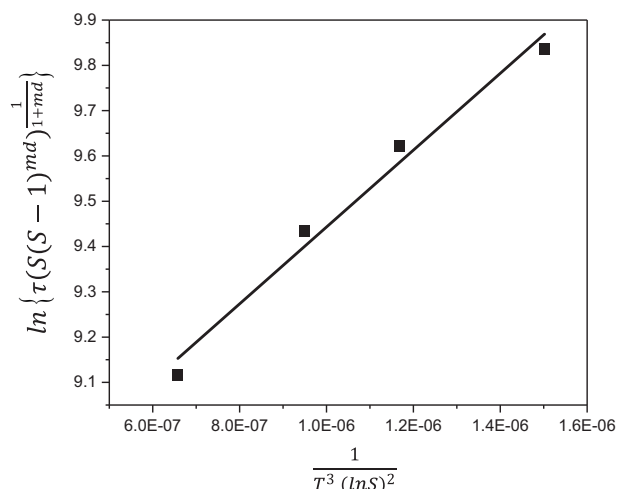


Figure 4. Induction time data to determine linear slope values for calculating the effective interfacial tension from data obtained for pABA in water solution at 6 g kg⁻¹ concentration.

mixed EtOH/H₂O solution. This study used TJM and the probability distribution method of induction time analysis, calculating an effective interfacial tension of 8.7 mJ m⁻². This provides some confidence in the results obtained through IbD, with values calculated to range from 2.11 to 8.39 mJ m⁻² for mixed EtOH:H₂O solutions studied through this methodology.

Examination of Eq. (3) reveals that an increase in the effective interfacial tension is consistent with an increase in the induction time, for a given supersaturation. However, from Tab. 1 it is clear that, for the IbD data, the effective interfacial tension increased with decreasing induction time. In this, the kinetic parameter, $\ln k_{\text{md}}$, would therefore have to be lower in order to be consistent with a decrease in induction time and also for the observed similar τ -versus- S behavior of the mixed-solvent IbD and pure-EtOH TJM systems. The calculated values of $\ln k_{\text{md}}$ are given in Tab. 1.

A decrease in $\ln k_{\text{md}}$ was calculated for the mixed-solvent solutions when compared to the pure EtOH and H₂O solutions, with the trend of decreasing $\ln k_{\text{md}}$ over the range of solution compositions studied through IbD also found to be consistent with an increase in effective interfacial tension. It should be noted that, although a negative $\ln k_{\text{md}}$ value was determined for the IbD mixed-solvent solution at 8 mol % EtOH, given the slight calculated error this is likely to be a very small positive value. From Eq. (4), it is clear that a decrease in $\ln k_{\text{md}}$ would be caused due to a decrease in α_{det} and/or an increase in one or more of the kinetic parameters in the denominator (z , f_e^* , c_s , and $f_{e,s}^{\text{md}}$). Unfortunately, it is not possible to quantify the changes in each of the kinetic parameters of $\ln k_{\text{md}}$ under the applied methodologies; however, estimations can be made as to the likely changes in values.

Given the lower solution concentrations studied through IbD, it can be confidently stated that there was a likely decrease in α_{det} . Nevertheless, given that the solution concentration of pABA in H₂O is one or two orders of magnitude lower than those of pABA in EtOH and in the mixed-solvent solution, it is clear that the kinetic parameters have a large effect on the

Table 1. Calculated values of effective interfacial tension and the CNT kinetic parameter, $\ln k_{\text{md}}$, for all solutions studied through TJM and IbD, alongside the induction times and supersaturation ranges for all solution compositions and concentrations.

Concentration [g kg ⁻¹]	Composition [mol % EtOH]	γ_{eff} [mJ m ⁻²]	$\ln k_{\text{md}}$	SE of $\ln k_{\text{md}}$	Induction time range [s]	Supersaturation range
<i>TJM ethanol solutions</i>						
180	100	0.85	6.66	0.18	40 260–3180	1.0–1.1
200	100	1.31	6.89	0.02	7700–3746	1.0–1.15
<i>TJM water solutions</i>						
6	0	2.1	8.59	0.09	41 631–15 405	1.2–1.3
8	0	2.6	6.96	0.20	20 064–3153	1.2–1.3
<i>IbD mixed solutions</i>						
104.3	31	–	–	–	4424	1.1
96.5	27	–	–	–	9751–133	1.1–1.15
88.9	24	2.32	1.34	0.52	1830–24	1.1–1.3
81.4	22	2.11	2.14	0.25	276–23	1.1–1.4
74.2	19	2.77	1.77	0.22	54–10	1.2–1.5
67.2	17	3.35	1.54	0.12	23–6	1.4–1.8
60.3	15	4.5	1.18	0.29	10–4	1.5–2.1
53.6	13	5.29	0.56	0.23	8–2	1.7–2.4
47	11	6.39	0.35	0.49	7–1	2.0–2.7
40.7	9	7.86	0.02	0.52	4–1	2.2–3.2
34.4	8	8.39	–0.22	0.35	4–1	2.6–3.7

SE denotes the standard error in results. Dashes indicate where data was not calculated, due to a limited number of data points obtained for a given solution composition.

induction time results. An increase in supersaturation is known to negligibly increase z , f_e^* , and $f_{e,s}^{\text{md}}$ [11], which would therefore be unlikely to be the contributing factor to the decrease in $\ln k_{\text{md}}$. The solution environment would also have an influence on f_e^* and $f_{e,s}^{\text{md}}$, given that they are controlled by the diffusion of solute molecules through the solution to the growing nuclei. pABA has been shown to be highly solvated by EtOH molecules, but very weakly solvated by H₂O molecules, with around twice the interaction energy calculated for EtOH interacting with a pABA molecule than for H₂O [10, 17]. Therefore, it would be expected that the pABA molecules in the mixed-solvent solutions would encounter less resistance to movement through the bulk solution to a nucleus, compared to pABA in EtOH solutions, meaning f_e^* and $f_{e,s}^{\text{md}}$ would have larger values. The low concentration of pABA in the H₂O solutions would limit the attachment frequency, and so these parameters would also be lower in value than the mixed-solvent solutions.

Furthermore, although it has been shown that c_s does not vary dramatically for pABA in solution with EtOH or H₂O [10], it is exponentially dependent upon supersaturation and is influenced strongly by the solution concentration [11], and as such would contribute to the lowering of $\ln k_{\text{md}}$ seen for the IbD results. Overall, given the solution effects highlighted above, it is expected that the kinetic parameters of pABA in the

mixed solutions studied through IbD would be larger than those of pABA in EtOH and H₂O solutions studied through TJM. It can be assumed that the larger kinetic parameters of the IbD solutions contribute to the similar τ -versus- S behavior of the mixed-solvent and EtOH solutions seen in Fig. 2, with the smaller kinetic parameters being responsible for the differing behavior observed for pABA in H₂O solutions.

Interestingly, the trend of the decreasing effective interfacial tension with increasing EtOH content for the IbD results, which follows the trend outlined by the solubility, suggests that it may be feasible to extrapolate the values of the effective interfacial tension from the mixed-solvent compositions (see black squares of Fig. 5) to pure-solvent solutions (see red circles of Fig. 5), shown by the exponential fitted dashed line in Fig. 5. However, such an extrapolation did not correlate with the pABA in H₂O solutions (see blue triangles in Fig. 5). This differential between the behavior of the two pure-solvent systems seems to follow a similar trend to that also observed in the τ -versus- S data (Fig. 2), where the data collected from IbD and from the pABA in EtOH solution from TJM show similar behavior, but not for the pABA in H₂O solutions. Clearly, more work is needed to fully understand this aspect.

Due to the large range of supersaturation studied through IbD, a change in nucleation mechanism from HEN to HON

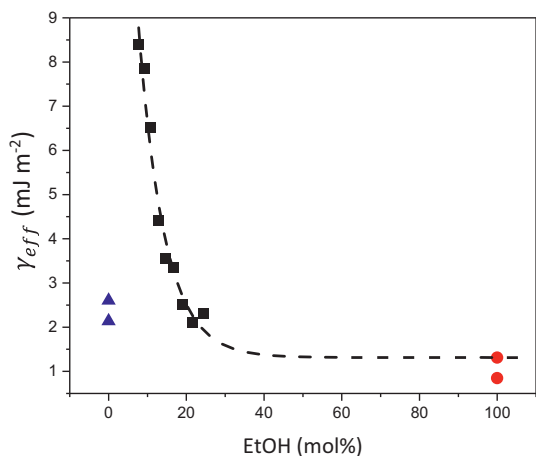


Figure 5. Calculated values of the effective interfacial tension from pABA in EtOH solutions at concentrations of 180 and 200 g kg⁻¹ (red circles) [6], pABA in H₂O solutions at 6 and 180 g kg⁻¹ (blue triangles), and IbD experiments over the full range of concentrations, compositions, and levels of supersaturation (black squares) [1]. The dashed line shows an exponential fit to the data collected through IbD with mixed solvent compositions.

was observed at a transition point of $S \approx 1.5$, with this level indicating a high enough driving force to nucleation to enable HON to occur. This mechanism change was determined through an observed change in effective interfacial tension through a plot of $(\log S)^{-2}$ versus $\log \tau$ and the relationship given in Eq. (8). The sharp change in the gradient of the linear

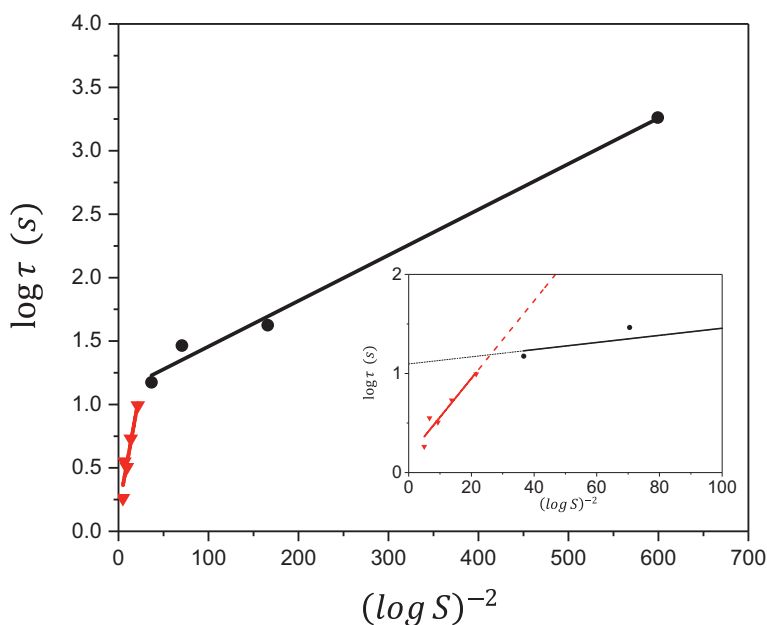


Figure 6. Induction time versus supersaturation for single-temperature and multiple-composition solutions of pABA in EtOH/H₂O mixtures for solutions at 299 K [1]. The inset highlights the region of mechanism change, with dashed lines showing the change in the slope intersect, indicating where the HEN-to-HON mechanism change occurred with increasing supersaturation.

correlation of the data in this plot demonstrates this mechanism change [14, 15], and is provided in Fig. 6. This insight into the nucleation of pABA in the solutions studied was attained through the IbD methodology but not through TJM, due to the limited range of supersaturations that could be accessed using the latter methodology, hence highlighting one of the critical benefits of the IbD methodology.

3.3.2 Critical Nucleus

Values of the critical cluster radius r^* and the number of molecules within the critical nucleus i^* calculated from induction time data from IbD for 81.4 g kg⁻¹ pABA in EtOH/H₂O 22:78 mol % solution and from TJM for 200 g kg⁻¹ pABA in EtOH solution and 6 g kg⁻¹ pABA in H₂O solution are displayed in Fig. 7. All results show a consistent trend of decreasing r^* and i^* with increasing supersaturation, reflecting the fact that an increased driving force enables a smaller critical nucleus size for nucleation. However, supersaturation was not found to be the only factor affecting the values of r^* and i^* , with the solution composition also impacting these values. This is evident in Fig. 6, with lower values of r^* and i^* determined for pABA in EtOH solution than for pABA in H₂O and mixed-solvent solutions, even at lower supersaturations.

The values of r^* and i^* for 81.4 g kg⁻¹ pABA in EtOH/H₂O 22:78 mol % solution and 6 g kg⁻¹ pABA in H₂O solution were found to be very similar across the overlapping range of supersaturations studied. This is due to the values of effective interfacial tension for the mixed EtOH/H₂O 22:78 mol % solvent solution and that of the H₂O solvent solution being 2.11 and 2.13 mJ m⁻², respectively, with similar temperature ranges studied. From Eqs. (6) and (7), it is clear that the parameters that effect the change in r^* and i^* across the range of solutions studied are the effective interfacial tension, the supersaturation, and the solution temperature. Thus, this comparison shows that, when the solution conditions are similar, regardless of whether the experimental methodology undertaken was IbD or TJM, pABA was found to nucleate in a similar manner, hence providing validity to the IbD results.

3.4 Advantages and Disadvantages of TJM and IbD

The temperature-jump methodology to determine the induction time enables key nucleation kinetic information to be obtained in a relatively simple way, involving rapid cooling to a set temperature followed by a temperature hold. This simplicity and capability have made it a very commonly used experimental methodology in the field of crystallization science and engineering. However, one drawback of TJM is that the levels of supersaturation that can be achieved by using it tend to be relatively low, creating a low driving force to nucleation, and as such the induction times can be quite

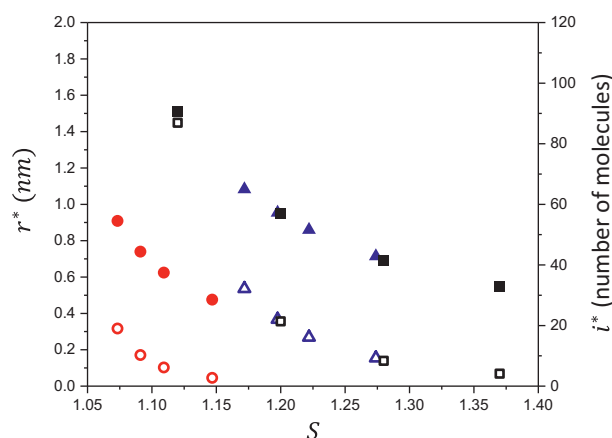


Figure 7. Critical nucleus radius (solid objects) and number of molecules within the critical nucleus (hollow objects) versus supersaturation from the data obtained through IbD and TJM. IbD data shown for 81.4 g kg^{-1} pABA in EtOH/H₂O 22:78 mol % solution (black squares/black hollow squares), TJM data for 200 g kg^{-1} pABA in EtOH solution (red circles/red hollow circles) and 6 g kg^{-1} pABA in H₂O solution (blue triangles/blue hollow triangles).

long as well as be subject to a large degree of variability. This means that a high number of experimental repeats is often required to obtain reproducible results and accurate and reliable kinetic data. Furthermore, this limitation in the achievable level of supersaturation means that it is not a suitable or viable method for accelerated nucleation testing, but it is able to provide a comparison and validation of results obtained through IbD over the overlapping range of supersaturation studied through both methodologies.

In contrast, the IbD methodology enabled a much greater range of supersaturation to be studied, and as such, through its use, accelerated nucleation testing can potentially be achieved. However, it does involve the addition of a second solvent to the system of study, which requires much more solubility data to be obtained over the full compositional range. Moreover, the final nucleation kinetic parameter results are obtained for mixed-solvent systems and not for the original single-solvent system that could be the system of interest, which requires accelerated nucleation testing. Nevertheless, the results shown in this study suggest that there is a link between the single-solvent system required to be accelerated and the mixed-solvent system for solutions of pABA in EtOH and H₂O. The addition of a second solvent also creates the necessity for calorimetry calibrations to offset the heat of mixing created upon antisolvent addition to a solution, which requires more experimental effort. The added experimental effort required through IbD can be somewhat offset by the lower number of repeats required to collect reliable and reproducible data at higher levels of supersaturation when compared to TJM.

However, in order for IbD to be an effective methodology for accelerated nucleation testing for predictive purposes, data collected at high levels of supersaturation have to be able to be extrapolated to low supersaturation. The current challenge with this is that the data collected over the range of supersaturations can involve a transition between nucleation mechanisms from

HEN to HON. Therefore, these two mechanisms need to be decoupled to allow for accurate extrapolations of results obtained, in order to ensure that each regime is not impacting on the extrapolation of the other. This is a current limitation, but statistical analysis of the data is being assessed to understand whether accurate predictions can be made through extrapolation of results from high to low supersaturation using IbD. Furthermore, a large number of industrial crystallization processes, particularly in pharmaceutical manufacturing, involve inducing high levels of solution supersaturation using an antisolvent methodology. Therefore, IbD represents a processing route that could enable a greater accuracy of kinetic information to be obtained in the early stages of product/process development as well as a more controlled crystallization methodology for large-scale production.

4 Conclusions

A comparison of two nucleation kinetic analysis routes was undertaken, with data collected from pABA in mixed EtOH/H₂O solutions using IbD and data collected for both pABA in EtOH solutions and H₂O solutions using TJM compared with respect to supersaturation, induction time, effective interfacial tension, critical nucleus size, and number of molecules within the critical nucleus.

Induction time data collected over a comparable range of supersaturation for IbD in mixed EtOH/H₂O solutions and the TJM results for pABA in EtOH solutions showed a similar trend, with similar values of induction time. In contrast, the results obtained for pABA in H₂O solutions from TJM showed the same trend in terms of non-linearly decreasing induction time with increasing supersaturation, but the values were offset, with regard to both the TJM results from pABA in EtOH solutions and the IbD results, with the induction time being larger for a given supersaturation. This “offset” of induction time values was consistent with the higher driving forces needed to overcome the higher effective interfacial tension value of H₂O when compared to EtOH and also reflected the weak solvation power of H₂O to pABA. In contrast, the solvation power of the mixed-solvent solution used with the IbD methodology appeared to be dominated by the stronger solvation abilities of the EtOH molecules, leading to a similar τ -versus- S trend for these systems.

The effective interfacial tension values calculated through IbD ranged from 2.1 to 8.4 mJ m^{-2} . In contrast, for the TJM experiments, the effective interfacial tension values ranged from 0.85 to 1.31 mJ m^{-2} for pABA in EtOH solutions and 2.1 to 2.6 mJ m^{-2} for pABA in H₂O solutions, depending on the solution concentration. This increased effective interfacial tension suggested that changes in kinetic parameters must be responsible for the aforementioned τ -versus- S data trends observed. An analysis of the kinetic parameters suggested that a decrease in α_{det} would occur with a lowering of the solution concentration with an increase in z , f_e^* , c_s , and $f_{e,s}^{\text{md}}$ likely for the IbD solutions studied, given the mixed-solvent environment and the higher levels of solution supersaturation achieved through this methodology. These changes were able to provide an explanation as to the τ -versus- S behavior of the TJM and IbD systems. A

comparison of results also showed that it may be possible to extrapolate values of the effective interfacial tension of the mixed-solvent solutions to the solutions containing only EtOH, with an exponential relationship. A comparison of results obtained for analysis of the critical nucleus, r^* and i^* , demonstrated that for all methodologies, r^* and i^* decreased non-linearly with increasing levels of supersaturation and that, over a similar range of effective interfacial tensions and supersaturations, the results were comparable. Overall, results obtained through TJM validated data collected through IbD over a similar range of supersaturation and provide confidence in the data collected at higher levels of supersaturation achievable through IbD.

In future work, TJM studies on mixed pABA in mixed EtOH/H₂O solutions, particularly to probe the detailed nature of the induction time offset observed between these two single solvents would be particularly useful. However, direct correlation of the two approaches over the full range of supersaturation studied through IbD is clearly not feasible, due to the limitations in achieving higher supersaturation through TJM. Furthermore, another interesting study would result from the use of IbD of a different system, such as a non-aqueous system, which would probe the applicability of IbD to a wide range of crystallization systems.

Acknowledgments

This research was carried out at the EPSRC Centre for Doctoral Training in Complex Particulate Products and Processes (EP/L015285/1), and forms part of the doctoral studies of one of us (P.L.K.) in collaboration with Infineum UK Ltd. and Syngenta UK Ltd., who we gratefully acknowledge for their support of this work. We also acknowledge the EPSRC (EP/IO14446/1 and EP/IO13563/1) for support of crystallization research at the University of Leeds.

The authors have declared no conflict of interest.

Symbols used

B	[-]	thermodynamic parameter of the classical nucleation theory
c	[m ⁻³]	absolute solute concentration
c^*	[m ⁻³]	saturation concentration
c_s	[m ⁻³]	solution concentration at the crystal solution interface
d	[-]	dimensionality of crystal growth
d_0	[m]	molecular diameter
f_e^*	[1 s ⁻¹]	frequency of monomers attachment to the nucleus at $\Delta\mu = 0$
$f_{e,s}$	[1 s ⁻¹]	frequency of molecular attachment per growth site at $\Delta\mu = 0$
i^*	[-]	number of molecules in the critical nucleus
J	[m ⁻³ s ⁻¹]	rate of nucleation
k	[J K ⁻¹]	Boltzmann constant
k_{md}	[-]	kinetic parameter of the classical nucleation theory

k_v	[-]	crystallite growth shape factor
m	[-]	crystallite growth exponent
r^*	[m]	critical nucleus radius
S	[-]	supersaturation
T	[K]	solution temperature
v_0	[m ³]	volume occupied by a solute molecule in a crystal
V	[m ³]	volume of the solution
V_c	[m ³]	crystallized volume
z	[-]	Zeldovich factor

Greek symbols

α_{det}	[-]	fraction of detectable crystallized volume
γ_{eff}	[m] m ⁻²	effective interfacial tension
τ	[s]	induction time to nucleation
τ_g	[s]	time for growth to a detectable size
τ_n	[s]	time to form a stable nucleus
τ_r	[s]	relaxation time for molecular cluster distribution

Abbreviations

CNT	classical nucleation theory
HEN	heterogeneous nucleation
HON	homogeneous nucleation
IbD	isothermal by design
pABA	<i>p</i> -aminobenzoic acid
TJM	temperature-jump isothermal methodology

References

- [1] P. L. Kaskiewicz, G. Xu, X. Lai, N. J. Warren, K. J. Roberts, C. Morton, P. Dowding, N. George, *Org. Process Res. Dev.* **2019**, *23*, 1948–1959.
- [2] S. Jiang, J. H. ter Horst, *Cryst. Growth Des.* **2011**, *11*, 256–261.
- [3] D. Mealey, D. M. Croker, Å. C. Rasmuson, *CrystEngComm* **2015**, *17*, 3961–3973.
- [4] D. M. Camacho Corzo, A. Borissova, R. B. Hammond, D. Kashchiev, K. J. Roberts, K. Lewtas, I. More, *CrystEngComm* **2014**, *16*, 974–991.
- [5] J. F. B. Black, P. T. Cardew, A. J. Cruz-Cabeza, R. J. Davey, S. E. Gilks, R. A. Sullivan, *CrystEngComm* **2018**, *20*, 768–776.
- [6] D. Toroz, I. Rosbottom, T. D. Turner, D. M. C. Corzo, R. B. Hammond, X. Lai, K. J. Roberts, *Faraday Discuss.* **2015**, *179*, 79–114.
- [7] J. W. Mullin, *Crystallization*, 4th ed., Butterworth-Heinemann, Oxford **2001**.
- [8] T. D. Turner, *Molecular Self-Assembly, Nucleation Kinetics and Cluster Formation Associated with Solution Crystallisation*, Ph.D. Thesis, University of Leeds **2015**.
- [9] *Crystal16*, Technobis, Alkmaar, **2020**. www.crystallization-systems.com/crystal16
- [10] T. D. Turner, D. M. C. Corzo, D. Toroz, A. Curtis, M. M. Dos Santos, R. B. Hammond, X. Lai, K. J. Roberts, *Phys. Chem. Chem. Phys.* **2016**, *18*, 27507–27520.

- [11] D. Kashchiev, *Nucleation*, Butterworth-Heinemann, Oxford **2000**.
- [12] K. Sangwal, *Additives and Crystallization Processes: From Fundamentals to Applications*, John Wiley & Sons, Chichester **2007**.
- [13] D. Kashchiev, A. Firoozabadi, *J. Cryst. Growth* **2003**, 250, 499–515.
- [14] O. Söhnel, J. W. Mullin, *J. Cryst. Growth* **1978**, 44, 377–382.
- [15] K. J. Kim, J. K. Kim, *Chem. Eng. Technol.* **2006**, 29, 951–956.
- [16] I. Rosbottom, C. Y. Ma, T. D. Turner, R. A. O'Connell, J. Loughrey, G. Sadiq, R. J. Davey, K. J. Roberts, *Cryst. Growth Des.* **2017**, 17, 4151–4161.
- [17] I. Rosbottom, J. Pickering, R. B. Hammond, K. J. Roberts, *Org. Process Res. Dev.* **2020**, 24, 500–507.